Mechanical Force Affects Expression of an In Vitro Metastasis-Like Phenotype in HCT-8 Cells

Xin Tang,[†] Theresa B. Kuhlenschmidt,[‡] Jiaxi Zhou,[¶‖] Philip Bell,[¶] Fei Wang,[¶‖] Mark S. Kuhlenschmidt,[‡*] and Taher A. Saif[†§*]

[†]Department of Mechanical Science and Engineering, College of Engineering, [‡]Department of Pathology, College of Veterinary Medicine, [§]Micro and Nanotechnology Laboratory, [¶]Department of Cell and Developmental Biology, The School of Molecular and Cellular Biology, and [‖]Institute for Genomic Biology, University of Illinois at Urbana-Champaign, Urbana, Illinois

ABSTRACT Cancer deaths are primarily caused by metastases, not by the parent tumor. During metastasis, malignant cells detach from the parent tumor, and spread through the circulatory system to invade new tissues and organs. The physical-chemical mechanisms and parameters within the cellular microenvironment that initiate the onset of metastasis, however, are not understood. Here we show that human colon carcinoma (HCT-8) cells can exhibit a dissociative, metastasis-like phenotype (MLP) in vitro when cultured on substrates with appropriate mechanical stiffness. This rather remarkable phenotype is observed when HCT-8 cells are cultured on gels with intermediate-stiffness (physiologically relevant 21–47 kPa), but not on very soft (1 kPa) and very stiff (3.6 GPa) substrates. The cell-cell adhesion molecule E-Cadherin, a metastasis hallmark, decreases 4.73 $\pm$ 1.43 times on cell membranes in concert with disassociation. Both specific and nonspecific cell adhesion decrease once the cells have disassociated. After reculturing the disassociated cells on fresh substrates, they retain the disassociated phenotype regardless of substrate stiffness. Inducing E-Cadherin overexpression in MLP cells only partially reverses the MLP phenotype in a minority population of the dissociated cells. This important experiment reveals that E-Cadherin does not play a significant role in the upstream regulation of the mechanosensing cascade. Our results indicate, during culture on the appropriate mechanical microenvironment, HCT-8 cells undergo a stable cell-state transition with increased in vitro metastasis-like characteristics as compared to parent cells grown on standard, very stiff tissue culture dishes. Nuclear staining reveals that a large nuclear deformation (major/minor axis ratio, 2:5) occurs in HCT-8 cells when cells are cultured on polystyrene substrates, but it is markedly reduced (ratio, 1:3) in cells grown on 21 kPa substrates, suggesting the cells are experiencing different intracellular forces when grown on stiff as compared to soft substrates. Furthermore, MLP can be inhibited by blebbistatin, which inactivates myosin II activity and relaxes intracellular forces. This novel finding suggests that the onset of metastasis may, in part, be linked to the intracellular forces and the mechanical microenvironment of the tumor.

INTRODUCTION

Metastasis, the spread of cancer cells from the primary tumor and invasion to new sites, is responsible for 90% of cancer mortality (1–3). Successful identification of metastasis-triggering signals is critical for the design of novel antimetastasis therapeutics. Unfortunately, the signals and associated molecular mechanisms regulating metastasis remain enigmatic to date (3–5). It has been long believed that, in addition to intrinsic genomic alterations of tumor cells, the progress of malignancy also can be driven by extrinsic microenvironment cues, such as matrix metalloproteinase proteases released by activated stromal cells (6,7), persistent inflammation associated with tissue wounding (8–11), and the loss of apicobasal polarity in surrounding epithelial cells (12,13). The relative contribution of these extrinsic and intrinsic cues, however, as well as the influence of the mechanical microenvironment on the regulation of tumor disassociation and metastasis, is not known.

Increasing evidence indicates the mechanical microenvironment plays a critical role in regulating tumor cell responses (14,15). Tumor cells sense, process, and respond to mechanical signals from their surroundings using a coordinated, hierarchical mechano-chemical system composed of adhesion receptors and associated signal transduction membrane proteins, the cytoskeleton, and molecular motors (5,16). For example, mammary epithelial cells form normal acinar parenchyma when cultured on substrates of physiological stiffness but display the structural and transcriptional hallmarks of a developing tumor when cultured on extracellular matrices (ECMs) of stiffness resembling tumor stroma (17). When in vivo proliferative and dormant breast cancer cells are cultured on two-dimensional in vitro plastic dishes, they readily proliferate regardless of their in vivo behavior. Surprisingly, when these same cells are grown in a three-dimensional culture matrix, they show distinct growth properties that correlate with their dormant or proliferative behavior at metastatic sites in vivo (18). There is no evidence, however, that shows a metastasis-like phenotype can be triggered by mechanical cues when cancer cells are cultured on a two-dimensional substrate in vitro. Here, and to our knowledge for the first time, we report experimental evidence indicating human colon carcinoma (HCT-8) cells can exhibit a metastasis-like phenotype (MLP) in vitro when cultured in the presence of an

Submitted August 5, 2010, and accepted for publication August 18, 2010.

*Correspondence: kuhlensc@illinois.edu or saif@uiuc.edu

Editor: Douglas Nyle Robinson.

0006-3495/10/10/2460/10 $2.00

doi: 10.1016/j.bpj.2010.08.034

appropriate two-dimensional mechanical microenvironment. The term, MLP, is used, because the cells exhibit several in vivo metastatic characteristics, such as dissociation from parent colonies, sustained proliferation and increased motility, downregulation of E-cadherin expression, reduction of cell adhesion (both specific and nonspecific) and the stable cell-state-transition (1–3,7,19–22). This in vitro metastasis-like phenotype raises the possibility that the in vivo mechanical-force balance between cellular structures and external microenvironment may serve as a signal to trigger the onset of metastasis.

MATERIALS AND METHODS

Cell culture

Human colon adenocarcinoma HCT-8 cells (Cat. No. CCL-244; ATCC, Manassas, VA) were cultured in RPMI 1640 (Cat. No. 23400-062; Gibco, Billings, MT) supplemented with 2 g sodium bicarbonate per liter, final concentrations of 10% horse serum (Cat. No. 26050-088; Gibco), 1× antibiotic-antimycotic (Cat. No. 15240-062; Gibco), and 1 mM sodium pyruvate (Cat. No. 11360; Gibco). Ma104 epithelial cells (embryonic African green monkey kidney) were obtained from Whittaker M.A. Bioproducts (Walkersville, MD) and cultured in MEM (Cat. No. 41500-018; Gibco) supplemented with 2 g HEPES per liter, 2.2 g sodium bicarbonate per liter, 1× antibiotic-antimycotic as above, and 5% fetal bovine serum (Cat. No. 16140; Gibco). (Please see the Supporting Material for methods to measure substrate stiffness and other details.)

RESULTS

Metastasis-like phenotype on 21–47 kPa gels

We examined human colon carcinoma (HCT-8) cells cultured on four substrates of different mechanical stiffness. Polyacrylamide (PA) gels were strategically prepared to have varying stiffness: 1.05 ± 0.17 kPa, 20.73 ± 1.03 kPa, and 47.05 ± 1.86 kPa, to mimic a wide range of physiological mechanical microenvironments (23,24). A quantity of 1.05 ± 0.17 kPa was used to mimic mammary gland, lymph node, brain, and breast tissues, with stiffness ranging from 0.1 to 2 kPa (17,24–26). A stiffness of 20.73 ± 1.03 kPa were used to mimic embryonic myocardium, muscle, lung, normal, and fibrotic human liver, with stiffness ranging from 9 to 25 kPa (27–31). A quantity of 47.05 ± 1.86 kPa was used to mimic in vivo cartilage (32,33). Because most routine cell culture is performed on polystyrene culture dishes (Elastic modulus: ~3.6 GPa), polystyrene served as the fourth substrate. All substrate stiffnesses were measured by an atomic force microscope (Asylum Research, Goleta, CA) (34) (see Fig. S1 in the Supporting Material). All substrates were functionalized with fibronectin or laminin ECMs. Two cell densities were used for culture, 150,000 cells/cm^2, and 50,000 cells/cm^2.

On 21 kPa and 47 kPa gels, HCT-8 cells attach to substrates, divide, adhere to each other, and form cell colonies (Fig. 1 *a*) in 2–4 days. Each colony consists of hundreds to thousands of well-attached cells, depending on initial seeding density. The colony size on 47 kPa gels is consistently larger than that on 21 kPa gels. On 1 kPa gels, cells do not spread but remain rounded, possibly due to a lack of traction (35,36), and occasionally form small colonies (Fig. S2 *a*). On hard polystyrene substrates, the cells reach 100% confluence by the end of two days (Fig. S3 *a*). After seven days of culture on 21 kPa and 47 kPa gels, mitotically competent and motile single cells begin to disassociate and migrate away from the cell colonies (Fig. 1 *b*). The dissociated cells lose their epithelial phenotype and display spherical shapes with a shape factor of 0.92 ± 0.03 (Fig. S5).

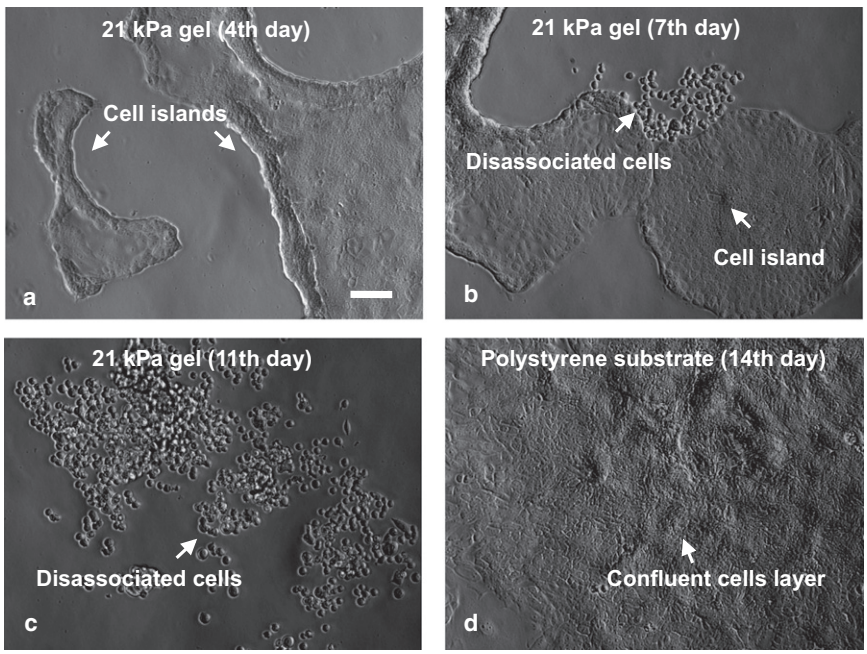

FIGURE 1 HCT-8 cells cultured on intermediate stiffness gel substrates (E = 21 kPa, coated with fibronectin) show metastatic-like phenotype (MLP). (*a*) Cells form cell colonies in 2–4 culture days. (*b*) Cells begin to dissociate from colonies on the seventh day. (*c*) An entire colony disassociates into individual cells in 11 days. (*d*) Cells form a confluent layer on hard polystyrene substrate (regular tissue culture petri dish, E = 3.6 GPa) and under the same culture condition as in panels *a*–*c*. They do not show MLP. Scale bar: 100 μm.

These cells also retain full viability when examined by dye exclusion live-dead assays (Fig. S4). Within two weeks of culture on 21 kPa gels, 70~90% of the cell colonies completely disassociate into numerous single cells (Fig. 1 *c*, Fig. 2 *d*, and Movie S2 in the Supporting Material). No cell disassociation was found on hard polystyrene substrates (Fig. 1 *d* and Fig. S3) or very soft 1 kPa gels (Fig. S2). The cell dissociation phenotype was observed on both fibronectin- and laminin-coated substrates, but the time to the onset of dissociation was different—seven days for fibronectin, and 15 days for laminin. MLP occurrence and time for its initiation is independent of original HCT-8 cell passage number; however, the use of lower passage HCT-8 cells resulted in a larger percentage of disassociated cells. At the seventh day of culture, 100% of the colonies dissociate from HCT-8 cells with passage 6, whereas only 5% of the colonies dissociate for cells with passage $\geq$43. However, after extended duration of culture, most colonies dissociate. Continuous video imaging (Fig. 2 and Movie S1) shows that once dissociation starts, it takes 5–10 h for the colony to be completely dissociated, a process that is much faster than that of colony formation (2–4 days). After disassociation, these cells extrude long filopodia (Fig. 2 *d*) and migrate away in a random fashion (Fig. 2 *a* and *b*). Their maximum migration speed measured was 0.9 $\pm$ 0.2 μm/min ($n = 25$). They come to a halt during cell division, after which the daughter cells remain associated on the top of the mother cell temporarily (Fig. 2 *c*, *insets*). Furthermore, the cell population increases dramatically after disassociation (Fig. 2, *c* and *d*). Normal, noncancerous epithelial (Ma104) or bovine endothelial cells cultured under the same conditions as described above, show cell colony formation, but no cell dissociation (Fig. S6).

MLP is inhibited by blebbistatin treatment

Blebbistatin was applied at 2, 5, and 10 μM concentrations after the HCT-8 cells were plated for 12 h on 21 kPa substrates. No cell dispersal was observed after nine days of culture with 5 and 10 μM concentration of blebbistatin, when 31.2 $\pm$ 7.2% of the untreated cell clusters (control) dissociate. Only ~4.6 $\pm$ 4.0% of the clusters dissociate with 2 μM blebbistatin after nine days of culture (see details in the Supporting Material and Fig. S10).

Cortex actin versus F-actin stress bundles

The three-dimensional actin cytoskeleton of HCT-8 cells was visualized using laser-scanning confocal microscopy after fixing and phalloidin-rhodamine immunocytochemical staining. We found that before dissociation, cell colonies on PA gels show well-defined actin networks near the substrate. The network spans the entire colony (Fig. 3 *a*1). HCT-8 cells in the uppermost layer of the cell colonies display cortical actin around the cell membrane, but no intracellular stress bundles (Fig. 3*a*3). Cells cultured on hard polystyrene substrates (which do not dissociate) show well-aligned actin stress bundles within individual cells (Fig. 3 *c*), implying large intracellular tension forces. This is expected from earlier studies which showed a correlation between substrate stiffness and intracellular forces as well as actin polymerization (37). After disassociation, HCT-8 cells on PA gels show

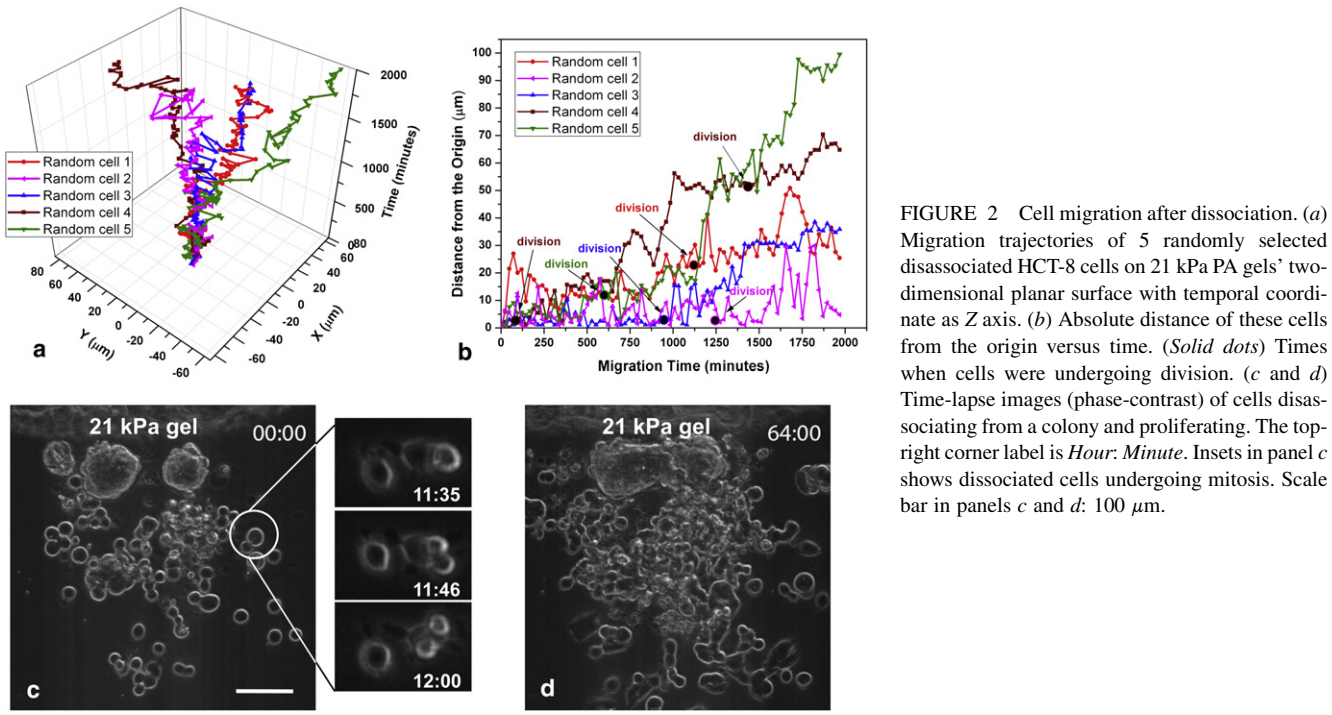

FIGURE 2 Cell migration after dissociation. (*a*) Migration trajectories of 5 randomly selected disassociated HCT-8 cells on 21 kPa PA gels' two-dimensional planar surface with temporal coordinate as *Z* axis. (*b*) Absolute distance of these cells from the origin versus time. (*Solid dots*) Times when cells were undergoing division. (*c* and *d*) Time-lapse images (phase-contrast) of cells disassociating from a colony and proliferating. The top-right corner label is *Hour*: *Minute*. Insets in panel *c* shows dissociated cells undergoing mitosis. Scale bar in panels *c* and *d*: 100 μm.

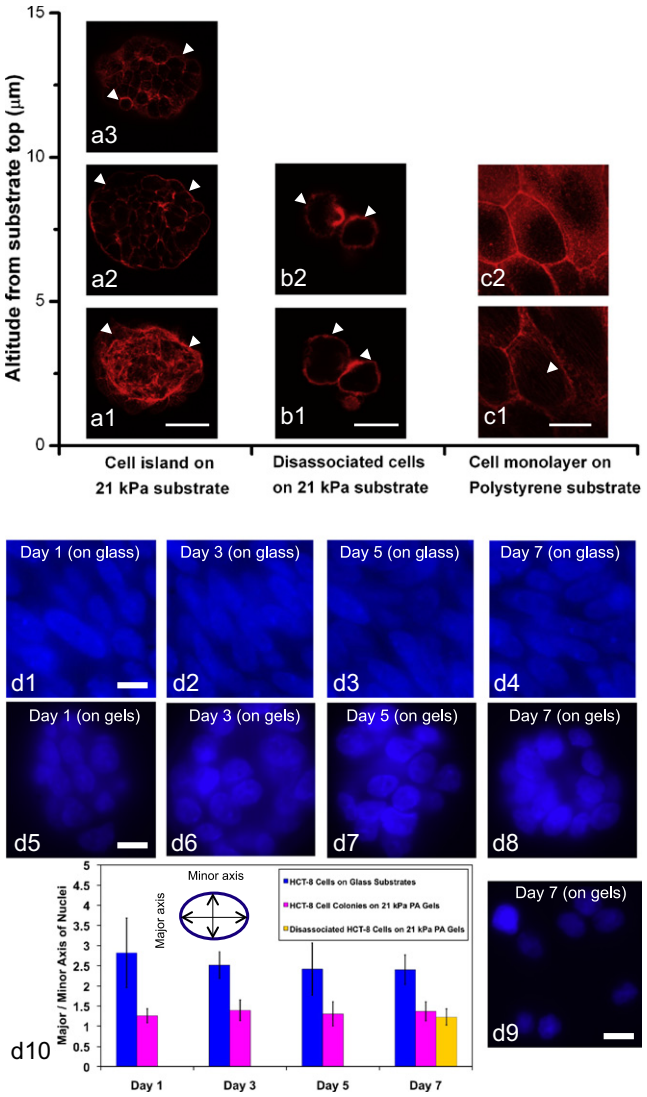

FIGURE 3 Confocal images of HCT-8 cells' actin cytoskeleton and the quantification of nuclear deformation of cells grown on 21 kPa gels and stiff polystyrene substrates. Actin network is diffuse and cross-cellular in HCT-8 cells on 21 kPa PA substrates. Well-defined and intracellular actin stress bundles are found in cells on hard substrates ($E = 3.6$ GPa). The cell nuclei on stiff polystyrene substrates are highly stretched compared to those on 21 kPa gels. The nucleus stretching is consistent with the actin cytoskeleton organizations and indicates that the intracellular tension force in cells on 21 kPa gels are lower than those in cells on stiff polystyrene substrates. (*a*) Cell colonies on 21 kPa gel substrates on fifth culture day (Scale bar: 25 μm). Intense cross-cellular F-actin filaments (indicated by *open arrowheads* in *a*1) are found at the cell colony bottom (*a*1). In contrast, as altitude increases, cells show only cortex actin (*open arrowheads*, panels *a*2 and *a*3 show different upper layers). (*b*) Disassociated HCT-8 cells on 21 kPa substrates on the seventh culture day (Scale bar: 15 μm). They only show cortex actin (*open arrowheads*) throughout the cell body, without any stress bundles. Panels *b*1 and *b*2 show cellular actin organization at different altitudes. (*c*) Cell monolayer on polystyrene substrates ($E = 3.6$ GPa) on seventh culture day (Scale bar: 20 μm) showing intracellular well-aligned actin stress bundles (*open arrowheads*, panel *c*1), implying large intracellular tension forces. Panel *c*2 shows the actin cytoskeleton of the same cell layer at higher elevation. (*d*) Panels *d*1–*d*8 show DAPI staining of nuclei of HCT-8 cells on 21 kPa gels and stiff polystyrene substrates on first, third, fifth, and seventh culture days. Panel *d*9 shows the dissociated cells with DAPI appearing on the seventh day. Scale bars: 10 μm. The nucleus-stretching factor is defined as the length ratio of elliptical nucleus major to minor axis (*d*10 *inset*, $n = 30$).

only cortical actin structures, and no actin stress bundles (Fig. 3 *b*), implying low intracellular and cell-substrate forces. These observations suggest that low intracellular forces exist in cells on 21~47 kPa substrates before dissociation compared to those experienced by monolayer cells in contact with a hard polystyrene or glass substrate. Surprisingly, disassociated HCT-8 cells when recultured on hard polystyrene substrates also show less filamentous actin (by 1.8 ± 0.1 times) than the original HCT-8 cultured under the same condition (Fig. S7).

Nucleus stretching on different stiffness substrates

Because the cell nucleus and actin filaments are physically linked (38), and the cell nucleus can be stretched by actin filament tension (39,40), we measured nuclear stretching using DAPI staining of HCT-8 cell nuclei in cells grown on both 21 kPa gels and stiff polystyrene substrates (Fig. 3*d*10). A nucleus stretching factor was defined as the length ratio of elliptical major axis/minor axis. We found that the nuclei in HCT-8 cells on stiff polystyrene substrates are stretched (Fig. 3 *d*1–*d*4) with a nucleus stretching factor (major/minor axis ratio) of 2.82 ± 0.86 (Day 1), 2.51 ± 0.33 (Day 3), 2.42 ± 0.65 (Day 5), and 2.40 ± 0.36 (Day 7). While on 21 kPa gels (Fig. 3 *d*5–*d*9), HCT-8 cells display less stretched and more circular-shaped nuclei, with a nucleus stretching factor of 1.26 ± 0.17 (Day 1), 1.39 ± 0.26 (Day 3), 1.31 ± 0.30 (Day 5), and 1.37 ± 0.24 (Day 7). These results indicate the intracellular forces on 21 kPa gels are lower than those on stiff polystyrene substrates.

E-Cadherin is reduced in dissociated cells

E-Cadherin is an essential cell-cell adhesion molecule. It has been consistently found that E-Cadherin expression decreases in metastatic cells (7,20). Therefore, it is, regarded as a clinically useful tumor malignancy marker. We examined the pattern of E-Cadherin immunofluorescent staining in colony-associated and disassociated HCT-8 cells. E-Cadherin in disassociated HCT-8 cells shows a weak pattern on the cell membrane (Fig. 4 *a*2). In colony-associated cells it appears as continuous and dense lines along cell-cell contact borders (Fig. 3 *a*1). Confocal microscopy was used to quantify the E-cadherin density per unit membrane area (see flow chart in Fig. S8). We found that the disassociated cells downregulate their surface E-Cadherin expression by 4.73 ± 1.43 times compared to their counterparts in cell colonies (Fig. 4 *a*). When the disassociated cells were harvested, recultured on hard polystyrene substrates,

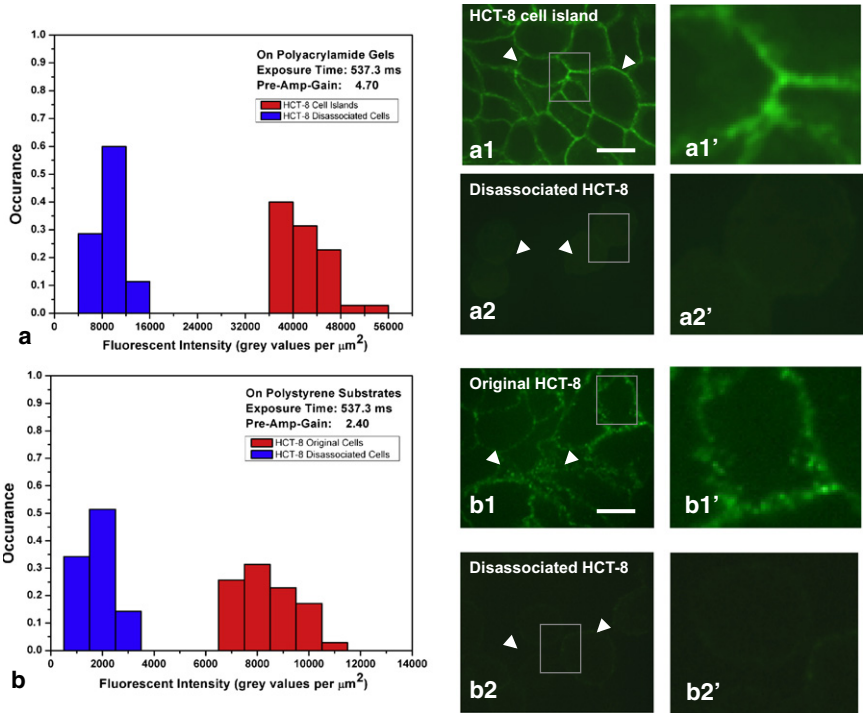

FIGURE 4 Dissociated cells have significantly lower E-Cadherin expression. (*a*) Histograms of E-Cadherin stain density per unit cell membrane area for HCT-8 cells on 21 kPa substrates on the seventh day of culture. The two histograms are for cells before and after dissociation. Panels *a*1 and *a*2 show confocal images of E-Cadherin stain of cells before and after dissociation, respectively. The open arrowheads in panel *a*1 indicate the continuous and dense E-Cadherin distribution along the cell-cell contact borders. The open arrowheads in panel *a*2 indicate a weak E-Cadherin staining pattern on the disassociated cells' membrane and the cell-cell contact regions. Panels *a*1′ and *a*2′ are the magnified views of the shaded squared areas in panels *a*1 and *a*2, respectively. (*b*) Histograms of E-Cadherin staining density per unit cell membrane area for original HCT-8 cells (not exposed to 21 kPa PA gels) and recultured disassociated HCT-8 cells (that had been cultured on 21 kPa PA gels for 14 days) on stiff polystyrene substrates (3.6 GPa) on the fourth culture day. The open arrowheads in panel *b*1 indicate the rich E-Cadherin presence along the cell-cell contact borders. The open arrowheads in panel *b*2 indicate a weak E-Cadherin pattern on the recultured disassociated cells' membrane. Panels *b*1′ and *b*2′ are magnified views of the shaded squared areas in panels *b*1 and *b*2, respectively. Scale bars: 10 μm. $n = 35$ for each histogram.

and their E-Cadherin expression reexamined (Fig. 4 *b*), we found they retained their downregulated surface E-Cadherin expression (by 4.86 $\pm$ 1.91 times) compared to the nondisassociated cells (Fig. 4 *b*1 and *b*2). These data imply that E-cadherin expression in the disassociated cells cannot be restored by reculturing on a stiff substrate.

Homotypic cell-cell adhesion rate is decreased after transition to MLP

Specific homotypic cell-cell adhesion rates for HCT-8 cells before and after plating on 21–47 kPa substrates (before and after disassociation) and normal Ma104 cells were compared using a Coulter counter assay as previously described (41). In all cases, the cells were harvested from either polystyrene or PA surfaces, individualized by trypsin treatment, and allowed to recover from trypsinization under the same incubation conditions before measuring intercellular adhesion rates (see the Supporting Material and Fig. S9) The Coulter counter measures the rate and extent of cell adhesion by quantifying the reduction in the number of single cells in suspension as cell aggregates form. Interestingly, disassociated HCT-8 cells (harvested from PA substrates) displayed a markedly lower extent and rate of cell-cell adhesion as compared to the original HCT-8 cells cultured on hard polystyrene substrates (Fig. 5 *b*). After 120 min of incubation, 84.8 $\pm$ 4.0% of the disassociated HCT-8 cells remained as single cells, in contrast to 37.6 $\pm$ 6.1% of original HCT-8 cells and 6.1 $\pm$ 0.4% of normal Ma104 cells (Fig. 5 *a*). Furthermore, this reduced cell-cell adhesion is independent of passage number. (Note that cells in suspension regain 40% of adhesion within 1 h and 80% within 3 h, and the rest of the adhesion takes ~18 h (42). The rate of adhesion is best measured within the first 3 h of suspension. It is this rate in which we are presently interested.) This rather remarkable result, showing the cell-cell adhesion capacity of HCT-8 cells is nearly absent after they disassociate from cell colonies, is also consistent with our finding of a pattern of reduced E-Cadherin expression (Fig. 4 *a*). Taken together, these results strongly support the hypothesis that HCT-8 cells downregulate cell adhesion molecules in response to mechanical cues they experience while growing on intermediate-stiff, but not very stiff, substrates. The reduction in cell adhesiveness was also seen when nonspecific adhesion forces between HCT-8 surfaces and SiO_2-coated Bio-MEMS probes were measured (Fig. 5 *c* and the Supporting Material).

The metastasis-like-phenotype is stable

To explore whether the HCT-8 cell transition to the MLP is reversible when cells are reexposed to hard substrates, we harvested the disassociated HCT-8 cells after 14 days of culture on 21 kPa PA gel substrates by two independent methods:

1. Trypsin treatment of the whole gel surface, and
2. Mechanical removal of the dissociated cells by gentle fluid shear.

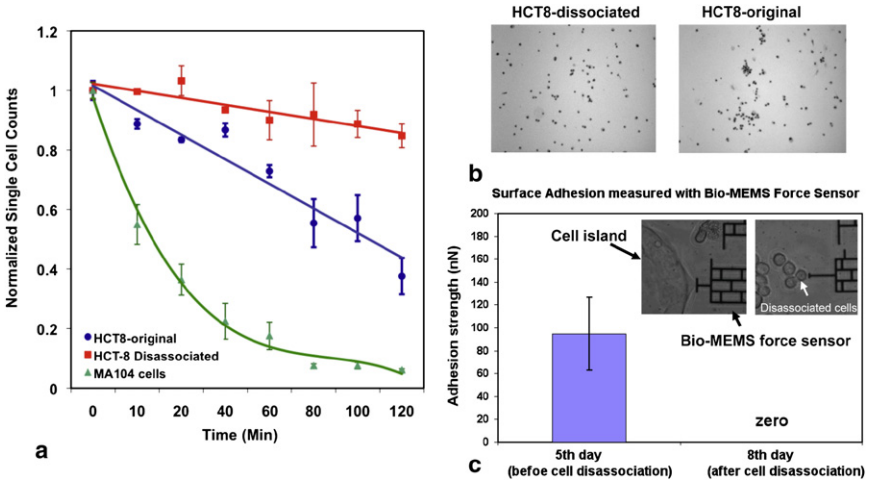

FIGURE 5 Disassociated cells have low cell-cell and nonspecific adhesion. (*a*) Comparison of cell-cell adhesion rates of original (not exposed to 21 kPa PA gels) HCT-8, disassociated HCT-8 cells harvested from 21 kPa PA gels, and normal epithelial Ma104 cells. (*b*) Photomicrographs of dissociated and original HCT-8 cells taken after 2 h of gyration followed by Coulter counter measurements (41). The relative absence of cell aggregates in the dissociated HCT-8 population is consistent with their low cell-cell adhesion rate shown in panel *a*. (*c*) Nonspecific adhesion measurement for both HCT-8 cell colonies (before disassociation) and disassociated HCT-8 cells on 21 kPa gels (67,68). $n = 12$ for both cell types (see details in the Supporting Material).

The cells were replated onto both fresh 21 kPa PA gels and hard polystyrene substrates. Surprisingly, we found the disassociated HCT-8 cells retain their disassociated phenotype regardless of the degree of stiffness of the new substrates and the method of harvesting (Fig. S11). This response to the substrate stiffness is completely opposite to that of the original HCT-8 cells maintained on polystyrene culture dishes (Fig. 1 *a* and Fig. S11). Besides the loss of response to substrate stiffness, the disassociated HCT-8 cells consistently maintained the disassociated phenotype after three additional passages in culture on polystyrene dishes. In addition, comparison of the E-Cadherin staining of both the original HCT-8 cells and harvested disassociated HCT-8 cells replated on polystyrene substrates showed a marked loss of E-Cadherin (reduced 4.86 ± 1.91 times) in the replated dissociated HCT-8 cells (Fig. 4 , *b*1 and *b*2). These results suggest that exposure of HCT-8 cells to the intermediate stiff mechanical microenvironment (21~47 kPa) has stably, perhaps irreversibly, locked them into a MLP that is more characteristic of a dissociative rather than associative (monolayer) or anchorage-dependent cell growth. While culture on hard substrates (polystyrene) preserved the original HCT-8 cells' associative cell growth phenotype typical of in vitro epithelial monolayers for >50 passages, a single exposure to PA substrate triggered these cells to transition to a new, dissociative, MLP cell state in only seven days. The results of these harvest-and-reculture experiments also imply that HCT-8 cells became disassociated in response to specific mechanical signals, rather than nonspecific degradation of local microenvironments during long-term in vitro culture.

Inducing E-Cadherin expression in MLP cells restores the non-MLP phenotype partially

To examine further the role of E-Cadherin in regulating the expression of MLP, we overexpressed E-Cadherin in MLP cells to explore whether the dissociated HCT-8 cells can form colonies again, i.e., whether the MLP can be reversed. For these experiments, we employed a lentivirus infection system to restore the E-Cadherin expression in dissociated HCT-8 cells displaying the MLP (see the Supporting Material and (43)). The majority (90–100%) of these dissociated HCT-8 cells were successfully transduced, as judged by expression of red fluorescent protein (Fig. 6 *a*1–*a*6). Western blotting experiments show that E-Cadherin protein expression in the virus-infected, dissociated HCT-8 cells was upregulated by ~3.58-fold (Fig. 6 *b*), which is equivalent or slightly higher than the amount of E-Cadherin expressed on original HCT-8 cells (Fig. 6 *e*). Approximately 60% of these cells displayed a somewhat flattened or epithelial shape (E cells) as compared to control dissociated HCT-8 displaying the MLP where >95% the cells were of the round form (R cells) when cultured on hard plastics (Fig. 6, *d* and *e*). The remaining 40% of these cells remain as R cells (Fig. 6 *d*3). In addition, unlike the original HCT-8 cells (Fig. 6*d*3), these E-Cadherin upregulated dissociated cells do not form the typical monolayers with merged cell boundary on hard polystyrene substrates, but remain as individual cells even as they grow to confluency (Fig. 6 *d*2). On 21 kPa PA gels, they partially form some clusters (Fig. 6*d*5), but the cells within the clusters seem to be separate from one another. These clusters are clearly distinct from those formed by original HCT-8 cells (Fig. 1 *a* and Fig. 6. 6 *d*6).

To explore further the effect of E-Cadherin upregulation, we compared homotypic cell-cell adhesion kinetics of dissociated HCT-8 cells with and without E-Cadherin upregulation. We found the rate of cell-cell adhesion increased nearly fivefold after E-Cadherin upregulation in dissociated HCT-8 cells, from −0.05 to −0.26 (Fig. 6 *c*). The extent of cell-cell adhesion, after 120 min of incubation, was 11.3 ± 4.4% for dissociated HCT-8 cells as compared to 52.8 ± 6.3% after E-Cadherin upregulation. The adhesion-rate regression analysis indicates that after E-Cadherin upregulation, 100% recovery of adhesion in HCT-8 R cells is reached

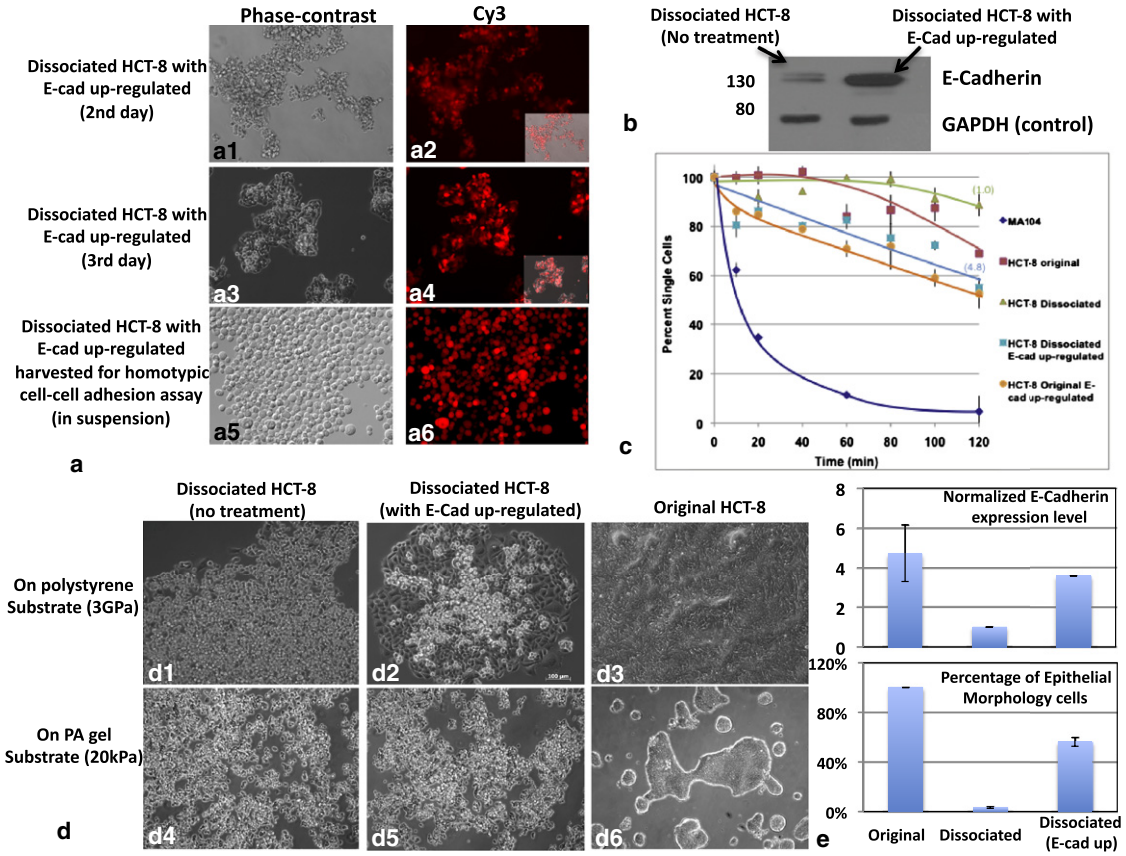

FIGURE 6 Inducing E-Cadherin expression in MLP cells partially restores the non-MLP phenotype. (*a*) The percentage of transduced dissociated HCT-8 cells is judged by expression of red fluorescent protein. The phase-contrast and fluorescent pictures of E-Cadherin upregulated cells at the second and third days after infection are shown in panels *a*1 and *a*2, and panels *a*3 and *a*4, respectively. The E-Cadherin upregulated dissociated cells harvested for Coulter counter adhesion assay is shown in panels *a*5 and *a*6. (*b*) Western blotting data shows the E-Cadherin content present in both not-treated and E-Cadherin upregulated dissociated HCT-8 cells with GAPDH as loading control. (*c*) Homotypic cell-cell adhesion rates of original HCT-8 (no treatment and E-Cadherin upregulated), dissociated HCT-8 (no treatment and E-Cadherin upregulated), and normal MA-104 cells (control). (*d*) Morphological patterns of dissociated HCT-8 (no treatment and E-Cadherin upregulated) and original HCT-8 cells (no treatment) on 21 kPa PA gels and stiff polystyrene substrates. (*e*) The normalized E-cadherin expression levels on original HCT-8 (no treatment; tested by fluorescent staining) and dissociated HCT-8 cells (no treatment and E-Cadherin upregulated; by Western blotting). The percentage of epithelial morphology cells versus overall cell populations in these three cell types, respectively. It shows after E-Cadherin in dissociated HCT-8 cells is overexpressed to close to that in original HCT-8, the MLP phenotype is partially restored to the non-MLP phenotype. Error bars represent standard deviations.

(cell adhesion rate $= -0.26$) compared to the original HCT-8 cells (cell adhesion rate $= -0.23$). A similar increase in cell adhesive rate and extent was also seen in the original, nondissociated HCT-8 cells after E-Cadherin upregulation (Fig. 6 *c*). These results indicate that while partial recovery of the E-cell phenotype and cell-cell adhesive activity occurs after restoration of E-Cadherin expression in dissociated HCT-8 cells, complete restoration of the E-cell phenotype likely requires multiple components in addition to E-Cadherin.

DISCUSSION AND CONCLUSIONS

The studies reported here describe a remarkable influence of the mechanical microenvironment on the behavior of HCT-8 colon cancer cells in vitro. Exposure of HCT-8 cells to PA gel substrates of appropriate mechanical stiffness triggers a profound stable transition, from an epithelial phenotype to a metastasis-like phenotype (MLP). The dissociated HCT-8 cells display a number of in vivo metastatic hallmarks: cell dissociation from parent colonies, sustained proliferation and increased motility, downregulation of E-Cadherin expression, reduction of cell adhesion (both specific adhesion rate and nonspecific adhesion strength), and the stable cell-state-transition (1–3,7,19–22). It is known that E-Cadherin is downregulated in most, if not all, epithelial tumors during the progression to tumor malignancy (7,20), and presence of E-Cadherin can strongly suppress the invasiveness of malignant cells (44,45). Our finding that E-Cadherin upregulation only partially restored the MLP in the dissociated HCT-8 cells suggests E-Cadherin may play a downstream rather than an initial signal transduction role in the mechanosensing cascade.

A number of reports have shown that normal tissue cells sense, adjust, and change their function in response to their mechanical microenvironment as much as they do in response to soluble chemical messengers (46–51). In particular, a mechanical-signal-mediated normal cell dispersal phenotype was reported in Guo et al. (52). Here, it is reported that clusters of normal cells in contact with very soft (4.41 ± 0.57 kPa) PA gel substrates remain as stable clusters. However, the clusters disperse and the cells dissociate from the clusters when they are in contact with stiffer substrates (12.40 ± 1.61 kPa PA gel or polystyrene substrates). This substrate stiffness-driven dispersal and durotaxis (53) have been hypothesized to originate from the competition between cell-ECM versus cell-cell signals. As the substrate stiffness increases, cell-substrate adhesion dominates over cell-cell adhesion, leading to cell dispersal. Durotaxis of normal cells toward the stiffer substrates has widely been observed and reported extensively by various groups (46,53–56). The dissociation of cancer cells from the cell clusters reported here is distinct from these earlier studies. In our studies, the HCT-8 cells first form clusters, and then disperse on the same soft substrate. Once dissociated, they no longer form clusters after replating on fresh soft or hard substrates—i.e., they lose their ability to sense substrate stiffness. To our knowledge, this type of mechanosensing phenomenon leading to a stable change in the MLP has not previously been reported in the literature.

Our finding raises an important question: How can a change in cell substrate softness induce such a stable metastatic phenotype?

Although the exact downstream signal pathways of MLP are yet to be discovered, integrins are believed to be one of the mechanosensors (57,58), because they transduce extracellular forces to intracellular cytoskeleton via focal adhesion complexes. The extracellular forces are in turn balanced and generated by forces within the cytoskeleton (51,59), powered by motor proteins such as myosin (37–39). The magnitude of the intracellular force depends on the actomyosin machinery, and how much pulling the external environment can resist (60). The harder the substrate, the higher are the intracellular forces (46). These forces may cause conformational changes in both the extracellular and intracellular components which may activate cryptic reaction sites, and initiate biochemical signaling cascades (47,61). Because the nucleus is connected to the cell cytoskeleton (38), intracellular forces are also transduced to the nucleus through long-distance force transmission (39) which may alter gene and protein expression (40,62), and a change in cell functionality. The long time (seven days of culture or 5–6 generations) required for the MLP transition of HCT-8 cells on 21~47 kPa substrates suggests a slow process, initiated by mechanotransduction and resulting in stable genetic changes. Inhibition of MLP by blebbistatin suggests that intracellular forces generated by myosin II play a role in the mechanotransduction pathway. Taken together, it appears that an appropriate amount of intracellular force, a consequence of the substrate softness, mediates the MLP.

Although the dissociated HCT-8 cells have many of the hallmarks of metastasis, such as low E-cadherin, low adhesion, stable cell-state transition, rapid and directed motility, and high cell proliferation, animal models will be essential for verifying their metastatic potential. There is, however, one experimental result suggesting that the dissociated HCT-8 cells might indeed be more metastatic. Two research groups (63–66) independently showed that during culture of HCT-8 cells in standard tissue culture flasks, a few rounded isolated cells (R cells) appear only on top of confluent epithelial monolayer (E cells). Although these studies did not relate the E to R transition with mechanical microenvironment in any form, we suspect that this transition might have been triggered by the soft environment of the apical surface of HCT-8 monolayer. We measured the micromechanical modulus of HCT-8 monolayer using AFM, and found it to be 3.39 ± 1.68 kPa (Fig. S1). Interestingly, the harvested R cells showed high metastatic invasiveness in both animal models and in vitro embryonic heart invasion assays (63,66).

In summary, our study raises the question whether the onset of in vivo metastasis is fundamentally linked with the tumor mechanical microenvironment—a paradigm that might have been largely overlooked in the understanding of cancer progression. If so, then soft cell culture substrates offer an attractive potential of developing in vitro metastatic models for both cancer drug screening and for mechanistic studies of the early phase of metastasis.

SUPPORTING MATERIAL

One equation, one table, 11 figures, and two movies are available at http://www.biophysj.org/biophysj/supplemental/S0006-3495(10)01029-5.

We thank Professors Mike P. Sheetz of Columbia University, Yu-Li Wang of Carnegie Mellon University, Geert Schmid-Schönbein of University of California at San Diego, and Douglas N. Robinson of Johns Hopkins University School of Medicine, for their insightful comments. We thank Mr. T. Cappa (Pathology, University of Illinois at Urbana-Champaign) for his assistance with cell culture and Coulter counter assays. Bio-MEMS force sensor was fabricated at the Micro and Nanotechnology Laboratory, University of Illinois at Urbana-Champaign. Staining and imaging were carried out at the Institute for Genomic Biology and Beckman Institute, University of Illinois at Urbana-Champaign with help from Dr. M. Sivaguru and Dr. D. Pan. Substrate stiffness characterizations were carried out with the help from Mr. S. MacLaren at the Materials Research Laboratory, University of Illinois at Urbana-Champaign.

This work was supported by National Science Foundation grants No. ECCS 07-25831 and No. 05-24675.

REFERENCES

1. Chambers, A. F., A. C. Groom, and I. C. MacDonald. 2002. Dissemination and growth of cancer cells in metastatic sites. *Nat. Rev. Cancer.* 2:563–572.

2. Weinberg, R. A. 2007. The Biology of Cancer. Garland Science, New York.
3. Gupta, G. P., and J. Massagué. 2006. Cancer metastasis: building a framework. *Cell.* 127:679–695.
4. Fidler, I. J. 2003. The pathogenesis of cancer metastasis: the 'seed and soil' hypothesis revisited. *Natl. Rev.* 3:453–458.
5. Ingber, D. E. 2008. Can cancer be reversed by engineering the tumor microenvironment? *Semin. Cancer Biol.* 18:356–364.
6. Vu, T. H., and Z. Werb. 2000. Matrix metalloproteinases: effectors of development and normal physiology. *Genes Dev.* 14:2123–2133.
7. Bissell, M. J., and D. Radisky. 2001. Putting tumors in context. *Nat. Rev. Cancer.* 1:46–54.
8. Sieweke, M. H., and M. J. Bissell. 1994. The tumor-promoting effect of wounding: a possible role for TGF-β-induced stromal alterations. *Crit. Rev. Oncog.* 5:297–311.
9. Dolberg, D. S., R. Hollingsworth, …, M. J. Bissell. 1985. Wounding and its role in RSV-mediated tumor formation. *Science.* 230:676–678.
10. Sieweke, M. H., N. L. Thompson, …, M. J. Bissell. 1990. Mediation of wound-related Rous sarcoma virus tumorigenesis by TGF-β. *Science.* 248:1656–1660.
11. Mintz, B., and W. K. Silvers. 1993. Transgenic mouse model of malignant skin melanoma. *Proc. Natl. Acad. Sci. USA.* 90:8817–8821.
12. Reichman, B. 1994. Oncogenes and epithelial cell transformation. *Seminar Cancer Biol.* 5:157–165.
13. Bilder, D., M. Li, and N. Perrimon. 2000. Cooperative regulation of cell polarity and growth by *Drosophila* tumor suppressors. *Science.* 289:113–116.
14. Weiss, L., and G. W. Schmid-Schönbein. 1989. Biomechanical interactions of cancer cells with the microvasculature during metastasis. *Cell Biophys.* 14:187–215.
15. Dong, C., M. J. Slattery, …, J. You. 2002. In vitro characterization and micromechanics of tumor cell chemotactic protrusion, locomotion, and extravasation. *Ann. Biomed. Eng.* 30:344–355.
16. Kumar, S., and V. M. Weaver. 2009. Mechanics, malignancy, and metastasis: the force journey of a tumor cell. *Cancer Metastasis Rev.* 28:113–127.
17. Paszek, M. J., N. Zahir, …, V. M. Weaver. 2005. Tensional homeostasis and the malignant phenotype. *Cancer Cell.* 8:241–254.
18. Barkan, D., H. Kleinman, …, J. E. Green. 2008. Inhibition of metastatic outgrowth from single dormant tumor cells by targeting the cytoskeleton. *Cancer Res.* 68:6241–6250.
19. Bacac, M., and I. Stamenkovic. 2008. Metastatic cancer cell. *Annu. Rev. Pathol. Mech. Dis.* 3:221–247.
20. Cavallaro, U., and G. Christofori. 2004. Cell adhesion and signaling by cadherins and Ig-CAMs in cancer. *Nat. Rev. Cancer.* 4:118–132.
21. Hirohashi, S., and Y. Kanai. 2003. Cell adhesion system and human cancer morphogenesis. *Cancer Sci.* 94:575–581.
22. Spaderna, S., O. Schmalhofer, …, T. Brabletz. 2008. The transcriptional repressor ZEB1 promotes metastasis and loss of cell polarity in cancer. *Cancer Res.* 68:537–544.
23. Wang, Y.-L., and R. J. Pelham, Jr. 1998. Preparation of a flexible, porous polyacrylamide substrate for mechanical studies of cultured cells. *Methods Enzymol.* 298:489–496.
24. Levental, I., P. C. Georges, and P. A. Janmey. 2006. Soft biological materials and their impact on cell function. *Soft Matter.* 3:299–306.
25. Miyaji, K., A. Furuse, …, S. Omata. 1997. The stiffness of lymph nodes containing lung carcinoma metastases: a new diagnostic parameter measured by a tactile sensor. *Cancer.* 80:1920–1925.
26. Miller, K., K. Chinzei, …, P. Bednarz. 2000. Mechanical properties of brain tissue in-vivo: experiment and computer simulation. *J. Biomech.* 33:1369–1376.
27. Mijailovich, S. M., D. Stamenović, …, J. J. Fredberg. 1994. Dynamic moduli of rabbit lung tissue and pigeon ligamentum propatagiale undergoing uniaxial cyclic loading. *J. Appl. Physiol.* 76:773–782.
28. Engler, A. J., M. A. Griffin, …, D. E. Discher. 2004. Myotubes differentiate optimally on substrates with tissue-like stiffness: pathological implications for soft or stiff microenvironments. *J. Cell Biol.* 166:877–887.
29. Cobbold, J. F. L., and S. D. Taylor-Robinson. 2008. Liver stiffness values in healthy subjects: implications for clinical practice. *J. Hepatol.* 48:529–531.
30. Masuzaki, R., R. Tateishi, …, M. Omata. 2007. Assessing liver tumor stiffness by transient elastography. *Hepatol. Intl.* 1:394–397.
31. Wu, Y., O. Cazorla, …, H. Granzier. 2000. Changes in titin and collagen underlie diastolic stiffness diversity of cardiac muscle. *J. Mol. Cell. Cardiol.* 32:2151–2162.
32. Li, L. P., M. D. Buschmann, and A. Shirazi-Adl. 2003. Strain-rate dependent stiffness of articular cartilage in unconfined compression. *J. Biomech. Eng.* 125:161–168.
33. Lyyra-Laitinen, T., M. Niinimäki, …, J. S. Jurvelin. 1999. Optimization of the arthroscopic indentation instrument for the measurement of thin cartilage stiffness. *Phys. Med. Biol.* 44:2511–2524.
34. Dong, R., T. W. Jensen, …, D. E. Leckband. 2007. Variably elastic hydrogel patterned via capillary action in microchannels. *Langmuir.* 23:1483–1488.
35. Pelham, Jr., R. J., and Y. Wang. 1999. High resolution detection of mechanical forces exerted by locomoting fibroblasts on the substrate. *Mol. Biol. Cell.* 10:935–945.
36. Yeung, T., P. C. Georges, …, P. A. Janmey. 2005. Effects of substrate stiffness on cell morphology, cytoskeletal structure, and adhesion. *Cell Motil. Cytoskeleton.* 60:24–34.
37. Wozniak, M. A., and C. S. Chen. 2009. Mechanotransduction in development: a growing role for contractility. *Nat. Rev. Mol. Cell Biol.* 10:34–43.
38. Maniotis, A. J., C. S. Chen, and D. E. Ingber. 1997. Demonstration of mechanical connections between integrins, cytoskeletal filaments, and nucleoplasm that stabilize nuclear structure. *Proc. Natl. Acad. Sci. USA.* 94:849–854.
39. Wang, N., J. D. Tytell, and D. E. Ingber. 2009. Mechanotransduction at a distance: mechanically coupling the extracellular matrix with the nucleus. *Nat. Rev. Mol. Cell Biol.* 10:75–82.
40. Thomas, C. H., J. H. Collier, …, K. E. Healy. 2002. Engineering gene expression and protein synthesis by modulation of nuclear shape. *Proc. Natl. Acad. Sci. USA.* 99:1972–1977.
41. Kuhlenschmidt, M. S., E. Schmell, …, S. Roseman. 1982. Studies on the intercellular adhesion of rat and chicken hepatocytes. Conditions affecting cell-cell specificity. *J. Biol. Chem.* 257:3157–3164.
42. Bosco, D., D. G. Rouiller, and P. A. Halban. 2007. Differential expression of E-cadherin at the surface of rat beta-cells as a marker of functional heterogeneity. *J. Endocrinol.* 194:21–29.
43. Zhou, J., P. Su, …, F. Wang. 2009. mTOR supports long-term self-renewal and suppresses mesoderm and endoderm activities of human embryonic stem cells. *Proc. Natl. Acad. Sci. USA.* 106:7840–7845.
44. Vleminckx, K., L. Vakaet, Jr., …, F. van Roy. 1991. Genetic manipulation of E-cadherin expression by epithelial tumor cells reveals an invasion suppressor role. *Cell.* 66:107–119.
45. Frixen, U. H., J. Behrens, …, W. Birchmeier. 1991. E-cadherin-mediated cell-cell adhesion prevents invasiveness of human carcinoma cells. *J. Cell Biol.* 113:173–185.
46. Discher, D. E., P. A. Janmey, and Y. L. Wang. 2005. Tissue cells feel and respond to the stiffness of their substrate. *Science.* 310:1139–1143.
47. Vogel, V., and M. Sheetz. 2006. Local force and geometry sensing regulate cell functions. *Nat. Rev. Mol. Cell Biol.* 7:265–275.
48. Engler, A. J., S. Sen, …, D. E. Discher. 2006. Matrix elasticity directs stem cell lineage specification. *Cell.* 126:677–689.
49. Georges, P. C., and P. A. Janmey. 2005. Cell type-specific response to growth on soft materials. *J. Appl. Physiol.* 98:1547–1553.
50. Folch, A., and M. Toner. 2000. Microengineering of cellular interactions. *Annu. Rev. Biomed. Eng.* 2:227–256.

51. LeDuc, P. R., and D. N. Robinson. 2007. Using lessons from cellular and molecular structures for future materials. *Adv. Mater.* 19:3761–3770.
52. Guo, W.-H., M. T. Frey, …, Y. L. Wang. 2006. Substrate rigidity regulates the formation and maintenance of tissues. *Biophys. J.* 90:2213–2220.
53. Lo, C.-M., H.-B. Wang, …, Y. L. Wang. 2000. Cell movement is guided by the rigidity of the substrate. *Biophys. J.* 79:144–152.
54. Byfield, F. J., Q. Wen, …, P. A. Janmey. 2009. Absence of filamin A prevents cells from responding to stiffness gradients on gels coated with collagen but not fibronectin. *Biophys. J.* 96:5095–5102.
55. Wong, J. Y., A. Velasco, …, Q. Pham. 2003. Directed movement of vascular smooth muscle cells on gradient-compliant hydrogels. *Langmuir.* 19:1908–1913.
56. Zaari, N., P. Rajagopalan, …, J. Y. Wong. 2004. Photopolymerization in microfluidic gradient generators: microscale control of substrate compliance to manipulate cell response. *Adv. Mater.* 16:2133–2137.
57. del Rio, A., R. Perez-Jimenez, …, M. P. Sheetz. 2009. Stretching single talin rod molecules activates vinculin binding. *Science.* 323:638–641.
58. Friedland, J. C., M. H. Lee, and D. Boettiger. 2009. Mechanically activated integrin switch controls $\alpha 5\beta 1$ function. *Science.* 323:642–644.
59. Esue, O., A. A. Carson, …, D. Wirtz. 2006. A direct interaction between actin and vimentin filaments mediated by the tail domain of vimentin. *J. Biol. Chem.* 281:30393–30399.
60. Bendix, P. M., G. H. Koenderink, …, D. A. Weitz. 2008. A quantitative analysis of contractility in active cytoskeletal protein networks. *Biophys. J.* 94:3126–3136.
61. Geiger, B., J. P. Spatz, and A. D. Bershadsky. 2009. Environmental sensing through focal adhesions. *Nat. Rev. Mol. Cell Biol.* 10:21–33.
62. Schlunck, G., H. Han, …, F. Grehn. 2008. Substrate rigidity modulates cell matrix interactions and protein expression in human trabecular meshwork cells. *Invest. Ophthalmol. Vis. Sci.* 49:262–269.
63. Rosenthal, K. L., W. A. F. Tompkins, …, W. E. Rawls. 1977. Variants of a human colon adenocarcinoma cell line which differ in morphology and carcinoembryonic antigen production. *Cancer Res.* 37:4024–4030.
64. Vermeulen, S. J., E. A. Bruyneel, …, M. M. Mareel. 1995. Transition from the noninvasive to the invasive phenotype and loss of alpha-catenin in human colon cancer cells. *Cancer Res.* 55:4722–4728.
65. Vermeulen, S. J., T. R. Chen, …, M. M. Mareel. 1998. Did the four human cancer cell lines DLD-1, HCT-15, HCT-8, and HRT-18 originate from one and the same patient? *Cancer Genet. Cytogenet.* 107:76–79.
66. Vermeulen, S. J., F. Nollet, …, M. M. Mareel. 1999. The αE-catenin gene (CTNNA1) acts as an invasion-suppressor gene in human colon cancer cells. *Oncogene.* 18:905–915.
67. Yang, S., and T. A. Saif. 2005. Micromachined force sensors for the study of cell mechanics. *Rev. Sci. Instrum.* 76:044301.
68. Yang, S., and M. T. Saif. 2007. Force response and actin remodeling (agglomeration) in fibroblasts due to lateral indentation. *Acta Biomater.* 3:77–87.